EJPMR, 2025, 12(11), 182-199 **Research Article** **Impact Factor 7.065**

EUROPEAN JOURNAL OF PHARMACEUTICAL AND MEDICAL RESEARCH

www.ejpmr.com

ISSN (O): 2394-3211
ISSN (P): 3051-2573
Coden USA: EJPMAG

EFFECTIVENESS OF THE TISSUE RESPONSE TECHNIQUE TO IMMEDIATE HYPOXIA: COMBINED USE OF CRYOLIPOLYSIS WITH CARBOXYTHERAPY IN THE FORMATION OF BEIGE ADIPOSE TISSUE AND ELIMINATION OF INFLAMMATORY FACTORS

[1]*Dr. Jairo Do Carmo Pirajá Junior, [2]Dr. Carlos Ruiz Da Silva

[1]Prof. Spec. PT, Dermatofunctional Physiotherapy Specialist. Faculdades Uninassau, Brasil).
[2]Prof. Phd, Msc, PT, / Faculdade CTA- Brasil; College of Int. Medicine and Aesthetics Harold Gillies, USA.

***Corresponding Author: Dr Jairo Do Carmo Pirajá Junior**

Prof. Spec. PT, Dermatofunctional Physiotherapy Specialist. Faculdades Uninassau, Brasil).

DOI: https://doi.org/10.5281/zenodo.17472374

How to cite this Article: *Dr Jairo Do Carmo Pirajá Junior, Dr. Carlos Ruiz Da Silva. (2025). EFFECTIVENESS OF THE TISSUE RESPONSE TECHNIQUE TO IMMEDIATE HYPOXIA: COMBINED USE OF CRYOLIPOLYSIS WITH CARBOXYTHERAPY IN THE FORMATION OF BEIGE ADIPOSE TISSUE AND ELIMINATION OF INFLAMMATORY FACTORS. European Journal of Pharmaceutical and Medical Research, 12(11), 182–199.

Article Received on 25/09/2025 **Article Revised on 15/10/2025** **Article Published on 01/11/2025**

ABSTRACT

Prolonged tissue hypoxia in mitochondrially deficient adipose tissue (white adipose tissue) is associated with several pathophysiological conditions, including chronic inflammation, obesity, microvascular complications, and diabetes. This prolonged oxygen (O2) deficiency in adipose tissue creates a microenvironment that favors inflammation, increased ghrelin and hypoxia-inducible factor (HIF), decreased electrical conduction in sympathetic nerve endings, and initiates cell survival paradigms. Apoptosis-resistant factors (BL1-XL and BCL2) prevail at the site. The induction of immediate hypoxia by freezing lipids through cryolipolysis, combined with elevated carbon dioxide (CO2) levels, which also generate immediate hypoxia in adipose tissue, activates the apoptosis of deficient cells and shifts the tissue environment to "thrive mode," resulting in increased blood flow, O2 supplementation, reduced inflammation, increased angiogenesis, mitochondrial crest formation, and activation of beige adipose tissue. Strategies using electrothermotherapy in aesthetics for body contouring increasingly incorporate systemic physiological manipulations combined with local application. In this study, in addition to demonstrating positive and impactful results with 100% satisfaction among those investigated, we demonstrated the true mechanism of action of these combinations through a literature review. The dual combination of cryolipolysis and carboxytherapy is effective and has already been used in more than 1,000 patients treated between 2022 and 2025, where the author uses the EUROICE terminology. The author explored a range of interventions designed to reduce visceral adipose tissue and prolonged inflammation, including cryolipolysis, carboxytherapy, and breathing exercises. The study involved 20 patients: 18 women and 2 men between the ages of 19 and 56, all with abdominal adipose tissue accumulation and hypotonia of the transverse muscle. An Immediate Hypoxia session was performed, followed by weekly sessions of 40 kHz ultrasound and functional electrical stimulation with breathing exercises. Before-and-after photographic comparisons of the protocol demonstrate visible and evident reductions in lipid deposits and correction of abdominal hypotonia. The treatment goes beyond aesthetic goals, offering a physiologically appropriate alternative for individuals unable to adhere to conventional training or surgical interventions. This treatment model promotes the transformation of white adipose tissue into beige adipose tissue and metabolic reprogramming, in addition to visible postural correction.

KEYWORDS: Cryolipolysis, Carboxytherapy, Body harmonization, weight loss, localized fat, low frequency ultrasound.

!-INTRODUCTION

Prolonged tissue hypoxia in mitochondrial-deficient adipose tissue (white adipose tissue) is associated with many pathophysiological conditions, including chronic inflammation, obesity, microvascular complications, and diabetes. This prolonged oxygen (O2) deficiency in tissue assemblies creates a microenvironment that supports inflammation and initiates cellular survival paradigms. The induction of immediate hypoxia by freezing lipids through cryolipolysis, combined with elevated tissue carbon dioxide (CO2) levels, activates apoptosis of deficient cells and shifts the tissue environment to "thrive mode," resulting in increased blood flow, added O2, reduced inflammation, and increased angiogenesis (Ruiz-Silva, 2025).

Cardiovascular and microvascular diseases can be caused by the chronic interruption of normal blood flow, which causes previously healthy tissues to cascade into a serious and sometimes permanent pathological condition. The condition caused by sustained hypoxia results in a slower metabolism, dependent on glycolytic pathways, and a chronic inflammatory state, perpetuated by an increased production of hypoxia-inducible factor 1α (HIF-1α). Multiple transcriptional responses to HIF-1α promote a survival response in cells, preventing cell death in response to continuous hypoxia (Kieras, 2021). In addition to cell survival, an important function of HIF-1α is the transcriptional activation of genes involved in the growth of new blood vessels and new adipocytes in an attempt to reverse this condition.

In contrast to the survival mode induced by severe or chronic hypoxia, immediate or transient hypoxia caused by increased metabolic demand in tissues results in an acute decrease in ATP stores, which is detected by cells through the action of adenosine monophosphate-activated protein kinase (AMPK) (Rodrigues, 2021). AMPK detects cellular energy status by monitoring the ATP:AMP ratio. When this ratio decreases, AMPK restores energy balance by inhibiting anabolic reactions that consume ATP and promoting catabolic processes that generate ATP. AMPK activation in vascular endothelial cells results in vasodilation and the growth of new blood vessels, increasing blood flow and oxygen delivery to the tissue, thus restoring normal tissue function (Rodrigues, 2021).

Tissue CO2 levels immediately increase in response to increased metabolic demand. Elevated tissue CO2 acts as a sensitive trigger for cellular responses to hypoxia, modulating biological signaling pathways (e.g., HIF-1α and AMPK) to restore normal tissue function and homeostasis.

Adipose tissue deposition in specific anatomical regions remains a challenge in both metabolic regulation and aesthetic approaches. Lipogenesis, an enzyme-regulated anabolic process, converts excess energy substrates, such as glucose and free fatty acids, into triglycerides stored in the cytoplasm of adipocytes. This mechanism, intensified by physical inactivity and hormonal imbalances, culminates in regional adipose tissue hypertrophy, often resistant to isolated caloric restriction or moderate aerobic activity (Lima; Vieira, 2017). Although often overlooked as aesthetic imperfections, these accumulations impact energy homeostasis and endocrine-metabolic function (Àvila, 2025).

Obesity and excess body fat have also been more recently associated with accelerated aging. In a study of over 1,000 people, obesity was found to increase biological age by up to 17% above chronological age (Correa-Burrows, 2022). Chronic inflammation associated with excess adipose tissue is believed to drive this increase in biological age, as chronic low-grade inflammation is a known hallmark of aging—one of the twelve cellular faults that accelerate the aging process (Franceschi, 2014; Loes-Otiz, 2023). In this study, those classified as obese also demonstrated evidence of other hallmarks of aging, including increased DNA damage and shorter telomeres (Correa-Burrows, 2022; Mundostock, 2015). Furthermore, several other studies have also demonstrated that obesity leads to other hallmarks of aging, including mitochondrial dysfunction (Tam, 2020), epigenetic alteration (Salvestrini, 2019), and senescence (Tam, 2020).

The weight-regulating hormone leptin is the antagonist of ghrelin, the orexigenic hormone that stimulates appetite. Research has shown that ghrelin-producing cells appear to be more abundant in morbidly obese and inflamed patients (Adamczak, 2013). Ghrelin is secreted in the stomach and inhibited by the satiety effects of leptin, which acts as a mechanism Hypothalamic-mediated feedback signaling. Intuitively, decreasing ghrelin and increasing leptin may be the apparent target of weight loss methods. However, there is a fine line between altering leptin/ghrelin concentrations and the hormonal imbalance that often precipitates weight gain. Unwarranted decreases in ghrelin and increases in leptin can also pose a health risk. Ghrelin is expressed in human T cells and monocytes to inhibit the expression of pro-inflammatory anorectic cytokines such as IL-1β and IL-6, which are implicated in chronic low-grade inflammation and aging (Ershler and Keller, 2000; Dixit, 2004). The regulation of inflammatory cytokines by normal ghrelin levels may be crucial in preventing inflammation.

Preadipocytes that undergo excessive apoptosis as they differentiate acquire relative resistance to apoptosis (Sorisky, 2000). Inhibitors of apoptosis (IAPs) act by suppressing apoptosis by inhibiting caspase activity.

Extracellular survival factors inhibit apoptosis through several pathways and bind to cell surface receptors, suppressing apoptosis. They stimulate increased production of antiapoptotic Bcl2 proteins, such as Bcl2 and Bcl-XL, activated by multiple adipogenesis (Ruiz-

Silva, 2024). Injury to sympathetic innervation, the absence of axonal nerve transmission, causes injury and blockage of the electrical bioconductivity of the SNS, activating hyperplasia, especially after vacuum compression and massage after cryolipolysis (Jalin, 2020; Strounza, 2018). Stimulation of nerve endings in the sympathetic system is necessary to generate beige adipose tissue. With a transient decrease in sympathetic neural input, preadipocytes can be activated (Seaman, 2016; Ho, 2017). Excessively hypertrophic white adipose tissue undergoes continuous necrosis, activating transcription factors (PPAR gamma), causing adipocyte hyperplasia, which generates compression of sympathetic innervation, hypoxia, and continuous inflammation of the adipose tissue (Martins; Ruiz-Silva, 2022; Ruiz-Silva, 2022; 2023; 2023).

MICOS deficiency leads to a coarser inner membrane architecture, and these mutations affect MICOS function and are responsible for a diverse spectrum of human diseases (Ruiz-Silva, 2023). Adipose tissue reduction is energy-dependent and can be achieved by reducing fat stores (lipolysis) or by permanent removal of adipocytes, necrosis, and apoptosis. Lipolysis is a metabolic process that degrades triglycerides present in adipose cells into their constituent molecules, glycerol and free fatty acids (FFA), through hydrolysis. (Ruiz-Silva, 2023; 2024).

Human brown adipocytes possess molecular attributes such as constitutive expression of UCP1, homogeneous multilocular morphology, and myogenic origin (Myf5+), while beige adipose tissue arises from non-myogenic progenitors (Myf52) under environmental stimuli, such as cold and exercise, and exhibits low levels of UCP1 expression under unstimulated conditions (Okla, 2017). Studies conducted by Dr. Lee between 2013 and 2016 demonstrated that cold exposure and exercise increase levels of the hormones irisin (produced by muscle) and FGF21 (produced by brown fat). In the laboratory, irisin and FGF21 can differentiate cells into beige adipose tissue cells over a six-day period (Loap, 2018). These two hormones, irisin and FGF21, are the primary signals that stimulate energy expenditure in the laboratory. Recent research suggests an inverse association between BMI and plasma irisin concentrations in morbidly obese individuals. In mammals, UCP1 BAT provides the primary mechanism for adaptive non-shivering thermogenesis to maintain body temperature in cold environments.

The use of cryolipolysis combined with microcurrents in the electrolipolysis mode

For transcriptional activation of UCP1, several transcriptional and co-regulatory factors are required, including PPARs and PGC1α (Dempersmier, 2015; Kelpert, 2017). However, the temperature range used to assess cold-induced thermogenesis represents another source of variability. The concept of cryoexposure is the use of local tissue cooling to control obesity. In cryolipolysis, apoptosis (hypoxia and reperfusion) is observed, with losses recorded over a long period (Manstein, 2008; 2009; Pugliese, 2020; Zelickson, 2009). Cryoexposure is a controlled method that uses cooling to induce lipolysis without inflammation (controlled by biochemical tests), a result generated by adaptive cryothermigenesis (Loap, 2018; 2022).

Exposure to environmental cold leads to a decrease in adipose tissue. When exposed to low temperatures, homeothermic mechanisms in humans include increased skin vasoconstriction to reduce heat loss and increased endogenous heat production, triggered by an increase in basal metabolic rate. Cold exposure also causes skeletal muscles to produce heat through muscle shivering-dependent thermogenesis, while muscle shivering-independent thermogenesis occurs in brown adipose tissue (BAT). Although the hypothesis of using cold exposure as a weight loss strategy was abandoned due to the belief that humans lacked brown adipose tissue, studies have shown that humans possess significant amounts of brown fat deposits, and the browning process can be stimulated by β3-AR receptor agonists (Ikeda, 2020).

Loap's recent publication brought to light the concept of weight loss with cryoexposure, based on the hypothesis of white fat conversion to brown tissue, which dates back over a century (Loap, 2018). Cold exposure increases energy and caloric expenditure through thermogenesis and fat metabolism (Loap, 2018). Despite the previous belief that brown adipose tissue was absent in humans, fluorodeoxyglucose imaging has shown the presence of large expansions of brown fat deposits (Loap, 2018). Evidence suggests that the conversion of white tissue to brown tissue is possible through the activation of BAT genes by transcription factors (Dempersmier, 2015). Daily serial cooling of abdominal adipose tissue results in progressive adipose tissue loss, confirmed by dual-energy X-ray absorptiometry, with no evidence of systemic inflammation, abnormal fat mobilization, or disruption of cellular integrity, necrosis, or death (Loap, 2018). Cryoexposure has been shown to reduce circumference and BMI without affecting inflammatory biomarkers, allowing daily applications (Loap, 2018). Lipid profile markers, including total cholesterol (TC), high-density lipoprotein (HDL), alanine aminotransferase (ALAT), alkaline phosphatase (ALP), aspartate aminotransferase (AST), gamma-glutamyltransferase (GGT), triglycerides (TG) and their relevant ratios, as well as thyroid hormones (TSH, total T4, and free T4), were also analyzed (Loap, 2018). Each cryoexposure application results in the extraction of 1,330 kcal via thermogenesis, as reported by Yoneshiro, Lans, and Le in 2013 (Loap, 2018). Cold-induced upregulation of UCP-1 O516 ZFP factors in low-temperature fat cells generates thermogenesis, allowing mitochondria to metabolize fat by beta-oxidation and generate heat (Dempersmier, 2015). Cold exposure also increases the expression of metabolic activity in beige tissue, leading to increased expression of the UCP-1

protein, which promotes thermogenesis and heat generation (Ikeda, 2020). The key to maximizing the effects of cryoexposure is to freeze as many areas as possible simultaneously and stimulate sympathetic nervous system receptors through electrolipolysis or electrostimulation to induce Zfp516 expression through sympathetic stimulation (contraction) by cold. Zfp516 binds to the PGC1a and Cox promoter regions, promoting transcriptional activation (Dempersmier, 2015). Intense contractions increase the expression of signaling proteins such as PPARγPGC-1α, which regulates mitochondrial biogenesis. Supramaximal contractions above 10 Hz and high magnetic flux density are most effective in activating PGC1α and inducing browning. These contractions stimulate anaerobic muscle fibers to undergo repetitive contractions, leading to high energy demand and a subsequent shift from aerobic to anaerobic metabolism. Peroxisome proliferator-activated receptor gamma-1 alpha (PGC1-alpha) is a transcriptional coactivator that plays a critical role in regulating energy metabolism and thermogenesis.

One of its primary its main functions are to induce browning of white adipose tissue (WAT), promoting the conversion of white adipocytes to brown adipocytes. This transformation involves the activation of thermogenesis mediated by uncoupling protein 1 (UCP1), which generates heat and increases metabolic activity in brown adipocytes.

The combination of cold and sympathetic nervous system stimulation through electrotherapy promotes the activation of the PERK and MICUS systems. The freezing action and simulation of physical activity through microcurrent (release of hormones similar to physical activity) after lipolytic stimuli (electrolipolysis) encounters an environment with many lipid droplets that influence the organization of cristae; mitochondria perform β-oxidation of fatty acids, but when stimulated by cold, drastic changes in morphology occur due to the activation of PERK (Gallardo-Montejano, 2021).

Cryolipolosis promotes the selective reduction of adipose cells. Histological analysis confirmed a selective and gradual reduction of adipose tissue through programmed death (apoptosis) triggered by reperfusion, the return of blood to the tissue by hypoxia activated by lipid freezing. The method's safety is highlighted by the absence of significant increases in liver enzymes or serum lipids (Ruiz-Silva, 2025).

Molecular studies demonstrated no changes in peroxisome proliferator-activated receptor (PPAR) transcripts. No changes in these transcripts were observed, highlighting the safety of the technology used (Ferraro, 2012).

Several physiological factors, such as temperature and exercise, have been shown to regulate the browning process. Maximal muscle contractions have been shown to activate PGC1-alpha, leading to increased mitochondrial biogenesis and oxidative metabolism. Maximal contractions cause a rapid and sustained increase in intracellular calcium levels, which activates calcium-dependent calmodulin kinase (CaMK); CaMK, in turn, phosphorylates PGC1-alpha. Maximal contractions promote the release of lactate and other metabolic intermediates that can activate AMP-activated protein kinase (AMPK), a key regulator of energy homeostasis that also activates PGC1-alpha.

Performing maximal contractions in environments with temperatures close to 0°C has been shown to be more effective in inducing browning compared to performing these contractions at room temperature. This is because cold exposure can activate the sympathetic nervous system and increase the secretion of norepinephrine, a hormone that stimulates lipolysis and activates mitochondrial thermogenesis, through the activation of β3-adrenergic receptors. Activation of β3-adrenergic receptors leads to the activation of AMPK, which in turn phosphorylates and activates PGC1-alpha. PGC1-alpha induces the expression of genes involved in mitochondrial biogenesis and oxidative metabolism, leading to an increase in mitochondrial thermogenesis and energy expenditure. In addition to its effects on thermogenesis, cold exposure can also activate the transient receptor potential cation channel member V, subfamily 1 (TRPV1), which is sensitive to low temperatures and is expressed in sensory neurons and adipose tissue. TRPV1 activation leads to the secretion of neuropeptide Y (NPY) and agouti-related protein (AgRP), two neuropeptides that stimulate food intake and reduce energy expenditure. However, TRPV1 activation in adipose tissue can also lead to the activation of mitochondrial thermogenesis through the activation of sympathetic nerves and the secretion of norepinephrine. In summary, performing submaximal and maximal contractions in environments with temperatures close to 0°C is more efficient in inducing browning than at room temperature, due to the activation of the sympathetic nervous system and the increased concentration of norepinephrine, which promotes the activation of MTD thermogenesis through the activation of β3-adrenergic receptors and the activation of PGC-1α. Furthermore, cold exposure can also activate the transient receptor potential subfamily V member 1 (TRPV1) cation channel, leading to the production of neuropeptides that stimulate food intake and produce energy expenditure.

Carboxytherapy Physiological Basis

Despite several publications demonstrating the effectiveness of carboxytherapy in reducing adipose tissue (Santos et al, 2020; Zago, 2020; Kill, 2020; Borba, 2021; Bastos, 2020; Alves, 2018; Moreira, 2020; Monteiro, 2021; Marinho, 2021; Lee, 2016; Kroumpouza, 2022; Kolodziejazak, 2018), none demonstrate the actual physiology capable of generating lipolysis. According to Milani, 2020, carboxytherapy is an invasive technique that uses medicinal carbon dioxide

(CO2), which is injected with an insulin needle into the subcutaneous tissue to stimulate physiological effects to improve circulation and tissue oxygenation. The Bohr effect is the main effect of carboxytherapy, as it acts on the vascular microcirculation of connective tissue, thus promoting vasodilation and increased nevolymphatic drainage (Reis et al, 2018; Farina et al, 2020). After a literature review, we conclude that CO2 activates angiogenesis not mediated by hypoxia-inducible factor 1a; CO2 is strongly anti-inflammatory; CO2 inhibits tumor growth and metastasis; and CO2 can stimulate the same pathways as exercise and, therefore, acts as a critical mediator in the biological response of skeletal muscle to tissue hypoxia.

This review presents data that highlight the potential use of CO2 as a therapeutic approach for tissue hypoxia, promoting tissue repair, reducing inflammation, reversing the pathophysiological effects of hyperglycemia, and generating lipolysis. Furthermore, it summarizes the state of knowledge regarding the cellular and molecular mechanisms underlying these beneficial effects of therapeutic CO2 administration.

In addition to its regenerative effects, CO2 has anti-inflammatory effects (Hanly, 2006; Howar, 1993). The key to the anti-inflammatory response using CO2 is the fact that it can penetrate and act directly on cells to modulate intracellular pathways that lead to inflammation and oxidative stress, as well as pathways linked to cell survival, proliferation, and apoptosis (Contreras, 2015). It is also relevant for patients with coronavirus disease 2019 (COVID-19), in which the viral spike protein of severe acute respiratory syndrome coronavirus 2 (SARS-CoV-2) binds to and disrupts the function of angiotensin-converting enzyme 2 (ACE2) on cell surfaces, leading to the activation of mitogen-activated protein kinases (MAPKs) and the production of pro-inflammatory cytokines (e.g., interferon-gamma, IL-1β, IL-6, and TNF-α) that cause pneumonia or ARDS (Galganska, 2021). Mechanisms of Action of Carbon Dioxide Therapy.

CO2/H+ concentrations and carbonic anhydrase govern CO2 sensing in the regulation of cellular function, with many of the findings relying on CO2 hydration and proton production to activate sensors and initiate a response. While hydration occurs spontaneously under physiological conditions, it occurs up to six orders of magnitude faster in the presence of the enzyme carbonic anhydrase (CA).[48] CO2 hydration through the action of CA is an important pathway for many responses. Although the relative importance of protons and CA is discussed in the context of the effect of CO2 on O2 release from hemoglobin in red blood cells, there are many additional responses where hydration is noted. The fact that it is not discussed does not mean that protons are unimportant. The role of protons is complicated by the fact that CO2 can affect protons extracellularly independently of how it affects protons intracellularly, indicating the importance of CA location. As more is discovered about the biology of CO2, the relative importance of protons and AC in sensing CO2 levels will come to light.

Increasing Blood Flow and Tissue Oxygenation

Increasing the CO2 concentration in tissue increases blood flow to that tissue (Xu, 2018; Matsumoto, 2016), and increased blood flow stimulates flow-mediated dilation of blood vessels (Ogoh, 2016; Hill, 2021). This vasodilatory action is partly due to CO2-induced NO production by the endothelium (which acts through the activation of cyclic GMP to relax the underlying smooth muscle), as it can be attenuated by inhibition of the endothelial NO synthase enzyme (Minamiyama, 2010).

An alternative mechanism for CO2-mediated increases in blood flow involves connexins and ATP release, which may act on ATP-sensitive potassium (KATP) channels in vascular smooth muscle to cause vasodilation, contributing to both resting blood flow and vasodilator-induced increases in blood flow. Connexins form large-pore channels that function as dodecameric gap junctions or hexameric hemichannels to allow the regulated movement of small molecules and ions across cell membranes. Hemichannels are a particularly important mechanism for ATP release in extracellular space (Dospinesw, 2019). CO2 binds to a carbamylation motif in connexins Cx26, Cx30, and Cx32, causing their hemichannels to open. Fluctuations in CO2 levels within the tissue alter their opening probability (Hill, 2016). Although direct CO2-dependent opening of the Cx26 hemichannel and subsequent ATP release have been shown to mediate an important part of neurovascular coupling (Hosford, 2022), it is possible that CO2 binding to endothelial Cx32 may explain the release of ATP into the blood in skeletal muscle during exercise, as the source of ATP remains to be defined (Kirby, 2013). CO2-mediated CGRP release and CA-dependent proton production can also activate K ATP channels in vascular smooth muscle (Brayden, 2002; Davies, 1990).

Finally, it has been demonstrated in the human forearm that there is an increased release of O2 from hemoglobin when CO2 is applied to the skin (TD) (Sakai, 2011). This CO2-driven elevation in tissue oxygenation can be explained by the Bohr effect, a rightward shift of the O2-hemoglobin dissociation curve with an increase in pCO2 or a decrease in pH (Bohr, 1904). This relationship was discovered in 1904 by Christian Bohr (Bohr, 1904), who showed that increasing CO2 tensions decreased the O2 affinity of whole blood in dogs. It should be noted, however, that Malte et al. showed that protons generated by CA have a greater effect on O 2 binding to hemoglobin than CO 2 itself (Figure 1) (Malte, 2018).

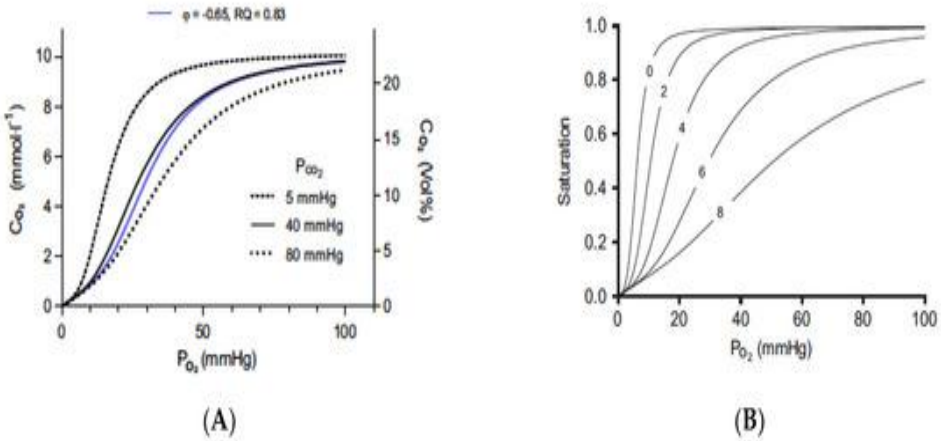

Figure 1. The Bohr effect as defined by CO 2 and protons. The Bohr and Haldane effects were modeled to describe the interactions between O 2 and CO 2 binding to hemoglobin (Malte, 2018). The Bohr effect describes how O 2 binding is decreased in the presence of CO 2 and protons. Graph (A) shows the traditional oxygen equilibrium curves (A) modeled under different CO 2 levels. The three black curves are the oxygen equilibrium curves obtained when the CO 2 partial pressure is held constant at the indicated values. The blue curve is obtained when CO 2 is added while oxygen is removed at a gas exchange rate, respiratory quotient (RQ), of 0.83. Graph (B) shows the effect of protons (B) on binding with a constant PCO 2 value of 40 mmHg and pH 7.2 at a PO 2 of 100 mmHg. Protons bind to Bohr groups on hemoglobin. The five oxygen equilibrium curves are obtained by increasing the number of bound Bohr groups (i.e., bound protons), as indicated by the numbers on the curves. pH is not shown because it is a poor indicator of proton binding. As protons bind to hemoglobin, pH increases. Figures reprinted/adapted with permission from Ref. (Malte, 2018). Copyright 2018, Journal of Applied Physiology.

There are two Bohr groups in each portion of hemoglobin, allowing a total of eight protons to interact with the hemoglobin molecule. In red blood cells, CO2 is rapidly interconverted into HCO3− and H+ ions via CA to generate the protons that can cause this effect. In the absence of CO2 and protons, hemoglobin will bind O2 until it reaches essentially anoxic tissue. Thus, tissues with low metabolism or that may be exposed to the body surface will have low CO2 levels and, therefore, will receive little O2 from the blood that may be flowing through the tissue. Raising CO2 to generate protons will force a rightward shift in the curves, so that O2 is released from hemoglobin and delivered to the tissue [Graph A]. The rightward shift caused by CO2 alone is relatively limited.

When external CO2 is applied, the CO2 is hydrated in the presence of CA, producing higher proton concentrations. The rapid hydration of CO_2 maintains the driving force for CO_2 diffusion into red blood cells and prevents CO_2 loss through conversion to HCO_2−. The effect of protons on oxygen binding is drastic, decreasing oxygen binding, as shown in Graph B. When hemoglobin binds protons during oxygen release, it acts as a buffer. The pH actually increases, so red blood cell pH is not a good indicator of proton binding to hemoglobin. According to Malte and Lykkeboe, "The Bohr effect is exerted by protons preloaded on Bohr groups at a given pH, as well as protons absorbed by Bohr groups during gas exchange. The proton preload sets the oxygen affinity (i.e., P50) at the onset of gas exchange. The protons absorbed during gas exchange lead to a further progressive decrease in oxygen affinity. The concerted effect of these two processes is very large, and the size of the Bohr effect has a direct influence on the oxygen affinity of hemoglobin." (Malte, 2018).

Enhancing Angiogenesis

While a single CO2 treatment can stimulate vasodilation and increase the release of O2 from hemoglobin due to the Bohr effect, repeated applications of CO2 maintain the tissue's O2 supply and induce angiogenesis (Xu, 2018; Xu 2017). Responses to CO2 include increases in basic fibroblast growth factor (Reglin, 2014; Nemeth, 2018), VEGF (Xu, 2018; Xu 2017), SIRT1 (Oe, 2018), PGC-1α (Wollina, 2004; Macura, 2020; Izumi, 2015; Irie, 2005), and NO (Xu, 2018; Xu 2017), all linked to neovascularization. Angiogenesis is a critical part of the healing process and is known to occur in response to tissue hypoxia. Hypoxia induces the transcription of angiogenic genes, such as VEGF, in part by stabilizing hypoxia-inducible transcription factors (Ferrara, 2003). A deficiency in blood flow leads to hypoxia, and elevated levels of CO2 accumulate in the tissue. Interestingly, although therapeutic CO2 introduction causes angiogenesis, it decreases or prevents HIF-1α production (Selfridged, 2016; Takemori, 2016). One mechanism for CO2-mediated HIF-1α suppression is through pH-dependent and O2-independent HIF-1α degradation.

Similarly, a non-HIF-mediated process can occur in skeletal muscle in response to exercise. Exercise generates high CO2 concentrations in skeletal muscle, and CO2 stimulates PGC-1α (Colfrey, 2016). PGC-1α is a hypoxia-induced metabolic sensor that regulates VEGF expression and angiogenesis in cultured muscle cells and

skeletal muscle in vivo (Arany, 2018). PGC-1α promotes angiogenesis through interaction with estrogen-related receptor alpha (ERRα), an orphan nuclear receptor that binds to the promoter region and a novel enhancer in the first intron of the VEGF gene to initiate robust VEGF gene activation in a HIF-independent manner (Arany, 2018; Hass, 2012; Yan, 2011). A reduced increase in VEGF expression in PGC-1α knockout mice after exercise demonstrates the functional relevance of this non-HIF-1α pathway in coordinating the angiogenic response to exercise (Hass, 2012).

The CO2 sensor that triggers the angiogenic process has not yet been defined. It was recently demonstrated that connexins bind CO2 (Dospinescu, 2019). Cx32 is expressed in endothelial cells and regulates angiogenesis, increasing tube formation and cell migration (Okamoto, 2004). It is conceivable that CO2 binding to Cx32 initiates neovascularization in response to chronic tissue hypoxia. An alternative candidate for a tissue CO2 sensor is ubiquitin. Although much of the control of angiogenic events is instigated by hypoxia-induced VEGF expression, the ubiquitin-proteasome system plays a central role in fine-tuning the functions of key proangiogenic proteins, including VEGF, VEGF receptors, angiogenic signaling proteins, and other non-VEGF pathways (Hahini, 2012). Ubiquitin is a highly conserved protein that regulates both protein activity and protein degradation through conjugation with target proteins (Hahini, 2012; Linthwaite, 2021). CO2 binds to lysine residues in ubiquitin, forming carbamate, and this reversible carbamylation reaction may be involved in the diverse physiological responses to fluctuating pCO2 levels. Linthwaite et al. described several sites where CO2 could bind to ubiquitin and alter its properties (Linthwaite, 2021). Deng et al. described how deubiquitination of AMPK is critical for its activation (Deng, 2016). AMPK is a crucial cellular energy sensor and is activated when intracellular ATP concentrations decrease and AMP or ADP concentrations increase in response to energetic or pathological stresses (Haldiez, 2012). AMPK activation plays a critical role in PGC-1α activation and therefore may be the link between CO2 and exercise to initiate non-HIF-mediated angiogenesis (Yan, 2011).

Reducing Inflammation

Some of the beneficial effects of therapeutic CO_2 may be related to its ability to suppress inflammatory signaling and increase ROS. Hypoxia, HIF-1α, and increased expression of glycolytic enzymes are associated with inflammation, and NF-κB can lead to increased HIF-1α expression. The loss of oxygen supply, energy depletion, and increased oxidative stress in ischemia/hypoxia result in reduced ATP synthesis and initiate a cascade of pathways that lead to cell death if not reversed. SIRT1 plays an important role in protecting against cellular stress and controlling metabolic pathways during ischemia/hypoxia.

CO_2 can trigger a specific repertoire of transcriptional events in a dose-dependent manner (Cummins, 2010). NF-κB is the master regulator of the sensing and signaling pathways that induce the transcription of multiple pro-inflammatory genes. As described in the studies mentioned above and others (Hanly, 2006; Cummins, 2010), CO2 can counteract inflammation to restore homeostasis. CO2 interrupts inflammation by binding to ubiquitin. Once CO2 is bound, ubiquitin will remodel and transform into a proteasome that will directly decrease the NF-κB response (Linthwaite, 2021; Keogh, 2017). During deubiquitination, ubiquitin is removed from a substrate to release its activity. This has been described as CO2-induced NFKB deactivation (Keogh, 2017). Adenyl cyclase stimulation: CO2 infusion into the subcutaneous tissue leads to a local increase in gas, which activates the enzyme adenyl cyclase. Increased cAMP: Activated adenyl cyclase generates an increase in the intracellular concentration of cAMP. Adipocyte lysis: The increase in cAMP initiates the lysis of triglycerides stored within the adipocyte, releasing free fatty acids and glycerol into the bloodstream. This process is known as lipolysis.

Carbon dioxide (CO2), used in the procedure, reacts with factors regulating tissue perfusion under physiological conditions. Carbon dioxide (CO2) is formed within cells as a result of cellular metabolism and then diffuses out of the cell. As a result, CO2 affects microcirculation in arterioles and precapillary vessels. As a result, tissue blood flow increases (KOLODZIEJCZAK et al., 2018). In adipose tissue, carbon dioxide (CO2) activates adenylyl cyclase. Furthermore, the effects of CO2 on adipose tissue can be direct or indirect. When carbon dioxide (CO2) has a direct lipolytic effect, there is a mechanical action mediated by the flow of gas injected into the hypodermis, without harming other tissues. The indirect effect of CO2 is related to the gas's ability to increase oxygen bioavailability for adipocyte metabolic activities, including fatty acid oxidative processes, reducing oxygen affinity for hemoglobin (DESSY, 2016).

II - MATERIAL AND METHODS

Fifteen patients of both sexes, aged between 25 and 50, were treated. They were diagnosed with excess abdominal adipose tissue and sagging abdominal muscles, especially the transversus abdominis muscle. All patients had clinical indications for cryolipolysis combined with microcurrent therapy, in addition to carboxytherapy. All patients were duly informed with the Informed Consent Form and signed an authorization for the use of their images, which was completed for diagnostic, scientific, and educational purposes.

Treatment performed

1. Cleansing the area to be treated with 2% aqueous chlorhexidine.
2. Use of an antifreeze blanket with a protective liner.
3. Use of microcurrents at 10 Hz with an intensity of 700 au.

4. Cryolipolysis freezing for 30 minutes at -11 degrees Celsius with a second 15-minute cooling cycle.
5. Use of 40 kHz ultrasound at 3.0 watts cm2, 2 minutes per head area, on all frozen tissue.
6. Finalization with Carboxytherapy, inflating the entire frozen area.

Weekly treatments were performed with 40 kHz ultrasound and functional electrostimulation combined with respiratory exercises for the transverse muscles.

III. RESULTS

Figures 2 to 16 show clinical cases treated with the protocol described above.

Figure 2: Patient J.F, Female, 40 years old.

Figure 3: Patient R.T.S J.F, male, 35 years old.

Figure 4: Patient M.A.S, female, 56 years old.

Figure 5: Patient R.F, female, 45 years old.

Figure 6: Patient L.S, female, 19 years old.

Figure 7: Patient A.F.J, female, 56 years old.

Figure 8: Patient S.F.A, female, 30 years old.

IV- DISCUSSION

Visual comparisons between pre- and post-intervention photographic records reveal evident reductions in subcutaneous fat volume, and a decrease in initial muscle hypotonia demonstrates extraordinary improvements in abdominal contour and skin tension, reporting complete satisfaction with the results. These results reflect not only apoptosis and reduction of local adipose tissue, but also the systemic metabolic reorientation promoted by the technique of immediate hypoxia and hyperoxygenation with CO_2, followed by a program of active muscle contraction and electrically induced muscle contraction. Previous reports identify the activation of AMPK triggered by FES and the subsequent mobilization of GLUT-4 as central processes in the increase in insulin-independent glucose uptake and fatty acid oxidation (Paul 2009), mechanisms likely replicated in this group.

The photographic documentation shows patients before the intervention, demonstrating a concentration of

adipose tissue in the infra- and supra-umbilical regions, as well as abdominal protrusion resulting from muscle hypotonia. Eight weeks after treatment, a reduction in subcutaneous volume, improvement in abdominal contour, and improved postural alignment were observed. The postural correction achieved in hypotonic individuals indicates that the respiratory and electrostimulation technique acts beyond acetylcholine metabolism and energy expenditure. By recruiting the deep transverse muscles, it promotes trunk stability and reduces abdominal protrusion, often misinterpreted as fat accumulation.

The results of the application of Cryolipolysis and Carboxytherapy using the immediate hypoxia technique induced with weekly low-frequency ultrasound treatments, followed by electrostimulation-assisted transverse muscle exercises, show consistent adipocyte attenuation. The effect of apoptosis initially generated by the hypoxia of Cryolipolysis, leading to the abandonment of mitochondrial cytochrome C and activation of procaspases 8 and 9, and inhibition of PPAR via the application of Carboxytherapy and potentiated by low-frequency ultrasound, this effect is consistent with the stimulation of apoptosis by low-frequency ultrasound previously described in controlled ex vivo models (Palumbo, 2011) and in vivo (Avila; Ruiz-Silva, 2025). Current visual evidence, although lacking histological verification, aligns with the expected morphological patterns of post-apoptosis body remodeling: smoother transitions between tissue planes, reduced bulging, and decreased localized lipid accumulation. These changes, which were far superior to surgical interventions and restrictive diets, suggest that mechanical fragmentation occurs at the cellular level, without visible inflammation or dermal compromise. In all 15 cases evaluated, volumetric reduction occurred without any recorded adverse cutaneous or circulatory effects.

Although the photographic method does not provide metric precision, the repeatability of visual results strengthens interpretive reliability (Ruiz-Silva, 2025).

Comparative studies corroborate the methodological framework for the use of cryolipolysis for adipose tissue reduction and weight loss (Ruiz-Silva, 2025). Pugliese et al. (2013) describe the occurrence of apoptosis after histological examination of adipocyte membranes under similar sonic protocols, while Honda et al. (2016) associate the use of 40 kHz ultrasound with a transient increase in free fatty acids (NEFA) without altering the lipid profile. These parallel findings corroborate the hypothesis that controlled ultrasound lysis promotes adipose apoptosis within physiological limits. Current clinical observations corroborate these conclusions. The intervention can affect metabolic flexibility, adipokine expression, and regional thermogenesis.

Functional electrical stimulation (FES), by inducing artificial muscle contractions, generates systemic biochemical effects. During contraction, AMPK, an enzyme sensitive to energy depletion, is activated, allowing the translocation of glucose transporters independently of insulin. Concomitantly, irisin, a myokine encoded by FNDC5, is released. Its action induces the phenotypic conversion of white adipocytes to beige cells via UCP1 expression, which intensifies thermogenesis and calorie expenditure (Pauli, 2009; Ruiz-Silva, 2023). Thus, FES ceases to be a mere toning tool and begins to act as a metabolic modulator (Ruiz-Silva, 2025).

Localized application of FES in areas of hypotonia, such as the abdomen, combined with specific breathing exercises for the transverse musculature, offers complementary responses. In muscles with low basal activation, electrical stimulation increases regional perfusion and promotes the oxidative use of fatty acids released by lipolysis (Martins, 2021). This metabolic redistribution supports the inclusion of FES in body contouring protocols, especially in patients individuals with restrictions on conventional exercise due to musculoskeletal limitations or chronic clinical conditions (Avila; Ruiz-Silva, 2025).

Immediate and transient hypoxia induction techniques with cryolipolysis and carboxytherapy, combined with beta-adrenergic stimulation, promote the biogenesis of mitochondrial cristae. Beige adipose tissue is a game-changer in the treatment of obesity and comorbidities due to its thermogenic and neurogenic effects (Martins; Ruiz-Silva, 2021; Ruiz-Silva, 2023; (Ruiz-Silva, 2024). Cold stress or beta-adrenergic stimulation activates PERK, which phosphorylates N-acetylglucosamine transferase (OGT). OGT phosphorylates TOM70 at Ser94, increasing the import of the MIC19 protein into mitochondria, promoting cristae formation and respiration. This activates the transformation of white adipose tissue (rich in lipids and poor in mitochondria) into beige adipose tissue (poor in lipids and rich in mitochondria) (Ruiz-Silva; 2024).

The endoplasmic reticulum (ER) kinase PERK is extremely sensitive to cold stress and stimuli from sympathetic nervous system (SNS), promoting the formation of mitochondrial cristae through increased mitochondrial import of MIC19, aided by TOM70 (Ruiz-Silva, 2023; 2024). Through cryolipolysis, the proliferation of healthy mitochondria is activated without the predominance of survival factors with anti-apoptosis proteins, through the mobile loop of cryolipolysis, generating the activation of the cristae organizing system MICOS through the translocation of the outer membrane translocation receptors MIC19 and 70. Beta-adrenergic stimuli also promote cristae biogenesis. The key is to alter this mitochondrial characteristic through fission (Yau, 2020; Martins; Ruiz-Silva, 2021; Ruiz-Silva, 2023; 2023). The combination of cold with sympathetic nervous system stimulation through electrotherapy promotes the activation of the PERK and MICOs. The

freezing action and simulation of physical activity through microcurrents (release of hormones similar to physical activity) after lipolytic stimuli (electrolipolysis) encounters an environment with many lipid droplets that influence cristae organization. Mitochondria perform the β-oxidation of fatty acids; however, when stimulated by cold, drastic changes in morphology occur due to the activation of PERK. (Gallardo-Montejano, 2021)

Crystal density increased dramatically after cold exposure, forcing the overexpression of perilipin 5 (PLIN(5). This increase in cristae density may be caused by PERK-dependent ER stress (Latorre-Muro et al., 2021).

Microcurrents or TCM, Cellular Microtherapy, consist of the application of low-intensity (μA) and low-frequency currents, similar to the endogenous electric fields generated during tissue repair systems (Ruiz-Silva, 2006; 2016; Xu, 2021) Microcurrent compensates for the bioelectricity that is decreased in hypoxic and inflamed tissues (Ruiz-Silva, 2006; 2016; Xu, 2021; Coy, 2022), generating ATP and mitogenesis. The presence of microcurrent generates a constant intensity current, increasing electrical flow, dissociating the water molecule, and forming hydrogen and hydroxyl ions around both electrodes. Hydrogen leads to the creation of ATP. It follows that, as a residual effect after the microcurrent stimulator is turned off, ATP production continues at the site. This ATP formation can be explained by Mitchell's chemiosmotic theory (Cheng, 1985; Ruiz-Silva, 2016).

Ruiz-Silva demonstrated that the number of superficial inflammatory cells decreased with increasing intensity of the applied low-frequency microcurrent, finding a statistically significant effect on the induction of lipolysis through stimulation of the postganglionic sympathetic neuron (Vilarinho et al. 2022; Couto; Ruiz-Silva; 2010).

The main purpose of the SNS is to stimulate the body's fight-or-flight response, remaining constantly active to maintain homeostasis (Motiejunaite et al., 2021). Microcurrent stimulation exerts "hormone-like effects," such as the secretion of norepinephrine in the postganglionic sympathetic neuron of the nervous system and in the G protein of the cell membrane (Al-Tubaikh, 2018). Norepinephrine secretion increases by binding to the β3-adrenoreceptor (β3-AR), which in turn converts ATP to cAMP in adipocytes (Noites, 2017).

The immediate hypoxia technique aims to reverse the effects of prolonged tissue hypoxia in adipose tissue with mitochondrial deficiency (white adipose tissue), reversing the pathological picture that includes chronic inflammation, obesity, microvascular complications, and diabetes. Using the immediate hypoxia and hyperoxygenation technique, we correct prolonged oxygen (O2) deficiency and inhibit cell survival factors.

In addition to cell survival, an important function of HIF-1α is the transcriptional activation of genes involved in the growth of new adipocytes. With the neovascularization promoted by this technique, we improve blood flow to supply more O2 to the tissue and reverse hypoxia, while activating the bioconductivity of the sympathetic nervous system.

In contrast to the survival mode induced by severe or chronic hypoxia, limited or transient hypoxia caused by increased metabolic demand in tissues results in an acute decrease in ATP stores, which is detected by cells through the action of adenosine monophosphate-activated protein kinase (AMPK). AMPK detects cellular energy status by monitoring the ATP:AMP ratio. When this ratio decreases, AMPK restores energy balance by inhibiting anabolic reactions that consume ATP and promoting catabolic processes that generate ATP. Activation of AMPK in vascular endothelial cells results in vasodilation and the growth of new blood vessels, increasing blood flow and oxygen supply to the tissue, thus restoring normal tissue function (Rodriguez, 2021).

The induction of immediate hypoxia by freezing lipids through cryolipolysis, combined with elevated tissue carbon dioxide (CO2) levels, activates apoptosis of deficient cells and shifts the tissue environment to "thriving mode," resulting in increased blood flow, oxygen supply, reduced inflammation, and increased angiogenesis and mitochondria. This study demonstrated efficacy in the 20 patients treated.

V- CONCLUSION

The induction of immediate hypoxia by freezing lipids through cryolipolysis, combined with high levels of carbon dioxide (CO2) in the tissues, activates the apoptosis of deficient cells and generates a shift in the inflamed tissue environment, with mitochondrial deficiency and low blood circulation, to "thriving mode," resulting in increased blood flow, added O2, reduced inflammation, and increased angiogenesis and mitochondrial crest formation, generating beige adipose tissue.

Freezing at low temperatures generates immediate hypoxia, initiating the apoptosis process by initiating the cytochrome c release cascade from the mitochondria and activating pro-apoptotic BH 123. Upon removal of the plaques, blood returns, which is blood reperfusion in the adipocytes, generating reactive oxygen species (oxidation) and activating apoptosis via the death receptor TNFα. Cryolipolysis promotes the selective reduction of adipose cells and is effective in treating dermal collagen remodeling. Concomitant with this effect, PERK is activated, which phosphorylates N-acetylglucosamine transferase (OGT), phosphorylating TOM70 at Ser94, increasing the import of the MIC19 protein into the mitochondria and promoting the formation of cristae and the formation of beige adipose tissue, rich in UCP1. Combined with CO2 infusion, in

addition to a new immediate hypoxia, we activate the inhibition of transcription factors, PPRA gamma, and generate a change in adipocyte typology, starting with the mitochondria and their organelles responsible for inhibiting apoptosis.

Strategies using electrothermotherapy in aesthetics for body contouring increasingly incorporate systemic physiological manipulations associated with local application. In this study, in addition to demonstrating positive and impactful results with 100% satisfaction among those investigated, we demonstrated the true mechanism of action of these combinations through a literature review.

VI-REFERENCES

1. Ruiz-Silva, C; Moleiro, D. Eficácia Do Uso Da Tecnologia De Criolipolise De Placas No Tratamento Da Flacidez Dermica Facial - Casos Clínicos. Aos., 2024; 2: 56-63.
2. Ruiz-Silva, C. Efeitos E Aplicações Da Eletrocrioexposição E Contrações Por Pulso Eletromagnetico De Alta Intensidade Para Indução De Browning. 16 Congresso Cientifico Internacional De Saúde Estética, 1 Edição. São Paulo, Triall Editorial, 2023.
3. Martins RAL, Matias M, Bueno FC De P, Oguri M, Leonardo PS, Ruiz-Silva C. Effects And Applications Of The High Intensity Electromagnetic Field (PEMF) In Health And Aesthetics: Perspectives And Clinical Evidence. Research, Society And Development, 2021; 10(14). DOI: 10.33448/Rsd-V10i14.2172
4. Ruiz-Silva, C; Moleiro, D; Ruiz-Silva, CR.- Treatment Of Lipedema Using Cryolipolysis Associated With Microcurrents; - IOSR Journal of Dental and Medical Sciences (IOSR-JDMS) e-ISSN: 2279-0853, p-ISSN: 2279-0861., October. 2024; 23(10)Ser., 7: 05-12. Doi-10.9790/0853-2310070512
5. Ruiz-Silva, C, Gomes-Lima, P; Ruiz-Silva, Kr; Moleiro, D. "Cellulite Treatment With Electrotherapeutic Combinations: Cryolipolysis, Microcurrents, Led And Ultrasound N" Iosr Journal Of Dental And Medical Sciences (Iosr-Jdms) E-Issn: 2279-0853, P-Issn: 2279-0861.Volume 23, Issue 10 Ser. 12 (October. 2024), Pp 22-30 Https://Www.Iosrjournals.Org/Iosr-Jdms/Papers/Vol23(10)/Ser-12/E2310122230.Pdf
6. Ávila, RRB; Ávila, LRB; Moleiro, D; Ruiz-Silva, C. Effectiveness Of The Combined Use Of Low-Frequency Electrostimulation With Low-Frequency Ultrasound: A Case Study. IOSR Journal of Dental and Medical Sciences (IOSR-JDMS) e-ISSN: 2279-0853, p-ISSN: 2279-0861.Volume 24, Issue 7 Ser., July. 2025; 7: 61-67.
7. Kierans, S.J.; Taylor, C.T. Regulation of glycolysis by the hypoxia-inducible factor (HIF): Implications for cellular physiology. *J. Physiol.*, 2021; *599:* 23–37. [Google Scholar] [CrossRef]
8. Rodríguez, C.; Muñoz, M.; Contreras, C.; Prieto, D. AMPK, metabolism, and vascular function. *FEBS J.*, 2021; *288:* 3746–3771. [Google Scholar] [CrossRef]
9. Adamczak M, Wiecek A The adipose tissue as an endocrine organ. Semin Nephrol, 2013; 33(1): 2-13. https://doi.org/10.1016/j.semnephrol.2012.12.008
10. Correa-Burrows P, Burrows R, Albala C Multiple events case-control study in a prospective cohort to identify systemic, cellular, and molecular biomarkers of obesity-induced accelerated aging in 30-years-olds: the ObAGE study protocol. BMC Geriatr, 2022; 22(1). https://doi.org/10.1186/s12877-022-03032-4
11. Cox EA, Nichols DS, Riklan JE Characteristics and Treatment of Patients Diagnosed With Paradoxical Adipose Hyperplasia After Cryolipolysis: A Case Series and Scoping Review. Aesthet Surg J., 2022; 42(12): NP763-74. https://doi.org/10.1093/asj/sjac219
12. Franceschi C, Campisi J Chronic inflammation (inflammaging) and its potential contribution to age-associated diseases. J Gerontol A Biol Sci Med Sci., 2014; 69: S4-9. https://doi.org/10.1093/gerona/glu057
13. López-Otín C, Blasco MA, Partridge L Hallmarks of aging: An expanding universe. Cell., 2023; 186(2): 243-78. https://doi.org/10.1016/j.cell.2022.11.001
14. Mundstock E, Sarria EE, Zatti H Effect of obesity on telomere length: Systematic review and meta-analysis. Obesity (Silver Spring), 2015; 23(11): 2165-74. https://doi.org/10.1002/oby.21183
15. Salvestrini V, Sell C, Lorenzini A Obesity May Accelerate the Aging Process. Front Endocrinol (Lausanne), 2019; 10. https://doi.org/10.3389/fendo.2019.00266
16. Tam BT, Morais JA, Santosa S Obesity and ageing: Two sides of the same coin. Obes Rev., 2020; 21(4). https://doi.org/10.1111/obr.12991
17. Dixit V, Schaffer E, Pyle R Ghrelin inhibits leptin- and activation-induced proinflammatory cytokine expression by human monocytes and T cells. J Clin Investig, 2004; 114(1): 57-66. https://doi.org/10.1172/JCI21134
18. HONDA, M. et al. Changes in blood biochemistry following localized fat reduction by low-frequency
19. Ershler WB, Keller TE. Age-associated increased interleukin-6 gene expression, late life diseases, and frailty. Annu Rev Med., 2000; 51: 245-270. https://doi.org/10.1146/annurev.med.51.1.245
20. Ávila, RRB; Moleiro, D; Ribeiro, BS; Scherner, B; Martelli, FP[5]; Ruiz-Silva, C ; Ávila, LRB - Body Blend Method – Integrated Electrotherapy Approach for Body Harmonization in 30 Days - *IOSR Journal of Pharmacy and Biological Sciences (IOSR-JPBS) e-ISSN:2278-3008, p-ISSN:2319-7676., Jul. – Aug. 2025; 20(4 Ser. 1): 15-18. www.iosrjournals.org*
21. PALUMBO, P. et al. Biological effects of low frequency high intensity ultrasound application on ex vivo human adipose tissue. *Ultrasound in Medicine & Biology*, 2011; 37(10): 1749–1759.

Disponível em: https://www.sciencedirect.com/science/article/abs/pii/S0301562911003314. Acesso em: 10 jul. 2025.
22. PAULI, J. R. et al. Exercise training and fasting activate SIRT1, increase PGC-1α activity, and induce mitochondrial biogenesis in muscle. *Applied Physiology, Nutrition, and Metabolism*, 2009; 35(4): 516–521. Disponível em: https://cdnsciencepub.com/doi/10.1139/H10-038. Acesso em: 10 jul. 2025.
23. PUGLIESE, R. et al. Histopathological features of tissue alterations induced by low-frequency ultrasound with and without saline solution infiltration. *Ultrasound in Medicine & Biology*, 2013; 39(9): 1637–1645. Disponível em: https://www.sciencedirect.com/science/article/abs/pii/S0301562913002293. Acesso em: 10 jul. 2025.
24. LIMA, V. A.; VIEIRA, R. P. Influência da obesidade na resistência à insulina e nas complicações metabólicas. *Revista Brasileira de Obesidade, Nutrição e Emagrecimento*, 2017; 11(65): 729–737. Disponível em: https://www.rbone.com.br/index.php/rbone/article/view/719. Acesso em: 10 jul. 2025.
25. Roberto, AE. Eletroestimulação: o exercício do futuro. São Paulo, Phorte Editora, 2006. ISBN 85.7655-083-0
26. Chen H, Yu Z, Liu N, Huang J, Liang X, Liang X, Liang M, Li M, Ni J. The efficacy of low-frequency ultrasound as an added treatment for chronic wounds: A meta-analysis. Int Wound J., 2023 Feb; 20(2): 448-457. doi: 10.1111/iwj.13893. Epub 2022 Jul 19. Retraction in: Int Wound J., Apr. 2025; 22(4): e70464. doi: 10.1111/iwj.70464. PMID: 35855676; PMCID: PMC9885464.
27. Voigt J, Wendelken M, Driver V, Alvarez OM. Low-frequency ultrasound (20-40 kHz) as an adjunctive therapy for chronic wound healing: a systematic review of the literature and meta-analysis of eight randomized controlled trials. Int J Low Extrem Wounds. 2011 Dec; 10(4): 190-9. doi: 10.1177/1534734611424648. Erratum in: Int J Low Extrem Wounds, Mar. 2012; 11(1): 69. PMID: 22184750.
28. Sorisky A, Bell A, Gagnon A. Tsh Receptor In Adipose Cells. Horm Metab Res., Nov-Dec. 2000; 32(11-12): 468-74. Doi: 10.1055/S2007 978672. Pmid: 11246811. 16.
29. Ruiz-Silva, C; Longo, B. Criolipolise De Placas E Microcorrentes: O Futuro Da Harminização Corporal. 5 Congresso Internacional Cientifico Multidisciplinar De Estética, 1 Edição. São Paulo, Triall Editorial, 2023.
30. Jain, Mohit, Et Al. "A 3-Dimensional Quantita T Ive Analysis Of Volume Loss Following Submen Tal Cryolipolysis."Aesthetic Surgery Journal, 2020; 40(2): 123-132.
31. Stroumza, N; Gauthier, N; Senet, P; Moguelet, P; Nail Barthelemy, R; Atlan, M. Paradoxical Adipose Hypertrophy (Pah) After Cryolipolysis. Aesthetic Surgery Journal, 2017; 38(4): 411–417.
32. Seaman, S. A; Tannan, S. C; Cao, Y; Peirce, S. M.; Gampper, T. J. Paradoxical Adipose Hyperplasia And Cellular Effects After Cryolipolysis: A Case Report. Aesthetic Surgery Journal, 2015; 36(1): Np6–Np13.
33. Ho, Derek, And Jared Jagdeo. "A Systematic Review Of Paradoxical Adipose Hyperplasia (Pah) Post--Cryolipolysis." Journal Of Drugs In Dermatology: Jdd., 2017; 16(1): 62-67.
34. Ruiz-Silva, C. Efeitos E Aplicações Da Eletrocrioexposição E Contrações Por Pulso Eletromagnetico De Alta Intensidade Para Indução De Browning. 16 Congresso Cientifico Internacional De Saúde Estética, 1 Edição. São Paulo, Triall Editorial, 2023.
35. Martins Ral, Matias M, Bueno Fc De P, Oguri M, Leonardo Ps, Ruiz-Silva C. Effects And Applications Of The High Intensity Electromagnetic Field (Pemf) In Health And Aesthetics: Perspectives And Clinical Evidence. Research, Society And Development, 2021; 10(14). Doi: 10.33448/Rsd-V10i14.2172
36. Ruiz-Silva Mr. Eficácia Do Uso Da Tecnologia De Criolipolise De Placas No Tratamento Da Flacidez Dermica Facial - Casos Clínicos. Aos., 2024; 2: 56-63.
37. Ferraro, G.A.; Francesco, F.; Cataldo, C.; Rossano, F.; Nicoletti, G.; D'andea, F. Efeitos Sinérgicos Da Criolipólise E Ondas De Choque Para Contorno Corporal Não Invasivo. Aesthetic Plast. Surg., 2012; 36: 666–679. [Google Scholar] [Crossref]
38. Pugliese, D.; Melfa, F.; Guarino, E.; Cascardi, E.; Maggi, M.; Ferrari, E.; Maiorano, E. Histopathological Features Of Tissue Alterations Induced By Cryolipolysis On Human Adipose Tissue. Aesthetic Surg. J., 2020; 40: 761–766. [Google Scholar] [Crossref]
39. Loap, S.; Lathe, R. Mechanism Underlying Tissue Cryotherapy To Combat Obesity/Overweight: Triggering Thermogenesis. J. Obes., 2018; 2018: 5789647. [Google Scholar] [Crossref]
40. Dempersmier, J. Et Al. Cold-Inducible Zfp516 Activates UCP1 Transcription To Promote Browning Of White Fat And Development Of Brown Fat., 2015.
41. Ikeda, K, Yamada. T. UCP1 Dependent And Independent Thermogenesis In Brown And Beige Adipocytes, 2020.
42. Kelpert, S. Et Al. Long-Term Cold Adaptation Does Not Require FGF21 Or UCP1, 2017.
43. Loap, S, Lathe, R. Mechanism Underlying Tissue Cryotherapy To Combat Obesity/Overweight: Triggering Thermogenesis, 2018.
44. Okla, M. Et Al. Dietary Factors Promoting Brown And Beige Fat Development And Thermogenesis, 2017.
45. Zelickson, Brian, Et Al. "Cryolipolysis For Noninvasive Fat Cell Destruction: Initial Results

From A Pig Model." Dermatologic Surgery, 2009; 35.10: 1462-1470.
46. Manstein, D.; Laubach, H.; Watanabe, K.; Farinelli, W.; Zurakowski, D.; Anderson, R.R. Selective Cryolysis: A Novel Method Of Non-Invasive Fat Removal. Lasers Surg. Med., 2008; 40: 595–604. [Google Scholar] [Crossref]
47. Pinto, H.; Arredondo, E.; Ricart-Jane, D. Evaluation Of Adipocytic Changes After A Simil-Lipocryolysis Stimulus. Cryo Lett., 2013; 34: 100–105. [Google Scholar]
48. Gallardo-Montejano Vi, Yang C, Hahner L, Mcafee Jl, Johnson Ja, Holland Wl, Fernandez-Valdivia R, Bickel Pe. Perilipin 5 Links Mitochondrial Uncoupled Respiration In Brown Fat To Healthy White Fat Remodeling And Systemic Glucose Tolerance. Nature Communications, 2021; 12(1): 3320. Doi: 10.1038/S41467-021-23601-2
49. Latorre-Muro P, O'malley Ke, Bennett Cf, Perry Ea, Balsa E, Tavares Cdj, Jedrychowski M, Gygi Sp, Puigserver P. A Cold-Stress-Inducible Perk/Ogt Axis Controls Tom70-Assisted Mitochondrial Protein Import And Cristae Formation. Cell Metabolism, 2021; 33(3): 598–614 E597. Doi: 10.1016/J.Cmet.2021.01.013
50. Lee, Hana, Et Al. "Bioelectric Medicine: Unveiling The Therapeutic Potential Of Micro-Current Stimulation." Biomedical Engineering Letters, 14.3(2024): 367-392.
51. Al-Tubaikh Ja Energy Medicine Internal Medicine: An Illustrated Radiological Guide (Second Ed)., 2018; 574–577. Springer. Berlin
52. Cheng N, Van Hoof H, Bockx E, Hoogmartens Mj, Mulier Jc, De Dijcker Fj, De Loecker W. The Effects of Electric Currents On Atp Generation, Protein Synthesis, And Membrane Transport Of Rat Skin. Clin Orthop Relat Res., 1982; 171: 264–272.
53. Motiejunaite J, Amar L, Vidal-Petiot E. Adrenergic Receptors And Cardiovascular Effects Of Catecholamines. Ann Endocrinol (Paris), 2021; 82(3–4): 193–197. Https://Doi.Org/10.1016/J.Ando.2020.03.012
54. Noites A, Moreira A, Melo C, Faria M, Vilarinho R, Freitas C, Santos R. Acute Effects Of Physical Exercise With Microcurrent In The Adipose Tissue Of The Abdominal Region: A Randomized Controlled Trial. Europ J Integrat Med., 2017; 9: 79–85. Https://Doi.Org/10.1016/J.Eujim.2016.11.001
55. Vilarinho R, Faria Sm, Monteiro Prr, Melo C, Santos R, Noites A (2022) Effects Of Abdominal Microcurrent In The Consumption And Proportion Of Energy Substrates During Aerobic Exercise: A Pilot Study. Healthcare. Https://Doi.Org/10.3390/Healthcare10050917
56. Couto, Miriam F., Cristina Melo, And Carlos Silva Ruiz. "Electrolipólise Mediada Por Tens E Microcorrente Em Associação Com Exercício Físico." I Congresso Internacional Da Saúde Gaia-Porto. Instituto Politécnico Do Porto. Escola Superior De Tecnologia Da Saúde Do Porto-Politema, 2010.
57. Farina, T. et al. Associação da carboxiterapia e intradermoterapia no tratamento da lipodistrofia localizada–Relato de caso. Revista Científica de Estética e Cosmetologia, 2020; 1(2): E0362021-4. https://doi.org/10.48051/rcec.v1i2.36
58. Reis, C. M. de. Et al (2018).. Avaliação temporal dos efeitos da carboxiterapia no tratamento da lipodistrofia localizada. Universidade do Vale do Taquari – UNIVATES, curso de biomedicina. Lajeado, novembro de 2018. RS. http://hdl.handle.net/10737/2635
59. Santos, É. L. et al O Uso da Carboxiterapia no Tratamento da Gordura Localizada. ID on line. Revista de psicologia, 2020; 14(53): 739-747. http://idonline.emnuvens.com.br/id
60. Zago, K. e Santos, J.R. 2020. Uso da Carboxiterapia Associada ao Princípio Ativo Cafeína no Tratamento da Lipodistrofia Localizada: Uma Revisão de Literatura / Use of Carboxiterapy Associated with the Caffeine Active Principle in the Treatment of Localized Lipodystrophy: A Literature Review. *ID on line. Revista de psicologia*, 2020; 14: 53(dez.), 1026–1033. DOI:https://doi.org/10.14295/idonline.v14i53.2809.
61. Milani, C.C. Efeitos da carboxiterapia como tratamento estético. Revista extensão, 2020; 4(1): 28-41. https://revista.unitins.br/index.php/extensao/article/view/3379
62. DESSY, Luca. Noninvasive Physical Treatments in Facial Rejuvenation. Internacional Textbook of Aesthetic Surgery, 2016. DOI: 10.1007/978-3-662-46599-87.
63. KOŁODZIEJCZAK, Anna; PODGÓRNA, Kasjana; ROTSZTEJN, Helena. Is carboxytherapy a good alternative method in the removal of various skin defects? Dermatologic therapy, 2018; e12699. DOI: 10.1111/dth.12699.
64. Kroumpouzos, George; Arora, Gulhima; Kassir, Martin; Galadari, Hassan, Wollina, Uwe; Lotti, Torello; Grabbe, Stephan., Goldust, Mohamad. Carboxytherapy in dermatology. Clinics in dermatology, 2022, 40(3):305-309. DOI: 10.1016/j.clindermatol.2021.08.020. LEE, Geórgia S.K. Quality survey on efficacy of carboxytherapy for localized lipolysis. Journal of Cosmetic Dermatology, 2016, 15: 484-492.
65. Marinho, P. Q. (2021). Carboxiterapiapara correção de erros estéticos. Health of Humans, v.3, n.2, p.38-52, 2021. DOI: http://doi.org/10.6008/CBPC2674-6506.2021.002.0005 Milani, C.C. Efeitos da carboxiterapia como tratamento estético. Revista extensão, 2020; 4(1): 28-41. https://revista.unitins.br/index.php/extensao/article/view/3379
66. Monteiro, E. M. O. et al Os efeitos da carboxiterapia associada a Drenagem Linfática no tratamento da lipodistrofia ginóide em mulheres. Revista Liberum

accessum, 2021; 13(1): 37-43. http://revista.liberumaccesum.com.br/index.php/RLA/article/view/133
67. Moreira, G M. Q e al (2020). Os benefícios da carboxiterapia no tratamento de lipodistrogia ginóide. Revista Multidisciplinar do Nordeste Mineiro, v1. 2020/01 ISSN 2178-6925 https://doi.org/10.17648/2178-6925-v1-2020-21.
68. Alves, D. et al. Efeito da Carboxiteparia no Tratamento do Fibro edema Gelóide-Revisão de Literatura. Revista Saúde em Foco, 2018; 10.
69. Bastos, G. R., & Nogueira, A. P. S. Os Benefícios da Carboxiterapia no Tratamento da Adiposidade Abdominal: Uma Revisão Integrativa. ID on line Revista de psicologia, 2020; 14(51): 157-167. DOI: 10.14295/idonline.v14i51.2564
70. Batista, S. et al Carboxiterapia associada à drenagem linfática manual na adiposidade abdominal. Fisioterapia Brasil, 2020; 21(3). DOI: https://doi.org/10.33233/fb.v21i3.3639 Boeff, et al. Gordura localizada, flacidez muscular e tissular - um estudo de caso. UNICRUZ. (s.d.) https://www.passeidireto.com/arquivo/104617188/gorduralocalizada-flacidez-muscular-e-tissular-um-estudo-de-caso
71. Borba, D. S. (2021). O uso da carboxiterapia nas disfunções estéticas. In Congresso Internacional em Saúde (No. 8). https://publicacoeseventos.unijui.edu.br/index.php/conintsau/article/view/19357
72. Kill, D. L. et al. (2020). A carboxiterapia no tratamento do fibroedema geloide. Tcc-Biomedicina. https://www.repositoriodigital.univag.com.br/index.php/biomedicina/article/view/486 Lucio, M. A.& MEJIA, D. P. M.. Eletrolipólise e Carboxiterapia para redução de gordura localizada. Manaus-AM. (s.d.)
73. Howard, M.; Muchamuel, T.; Andrade, S.; Menon, S. Interleukin 10 protects mice from lethal endotoxemia. *J. Exp. Med.*, 1993; *177:* 1205–1208. [Google Scholar] [CrossRef] [PubMed]
74. Hanly, E.J.; Fuentes, J.M.; Aurora, A.R.; Bachman, S.L.; De Maio, A.; Marohn, M.R.; Talamini, M.A. Carbon dioxide pneumoperitoneum prevents mortality from sepsis. *Surg. Endosc*, 2006; *20:* 1482–1487. [Google Scholar] [CrossRef] [PubMed]
75. Contreras, M.; Masterson, C.; Laffey, J.G. Permissive hypercapnia: What to remember. *Curr. Opin. Anaesthesiol*, 2015; *28:* 26–37. [Google Scholar] [CrossRef] [PubMed]
76. Galganska, H.; Jarmuszkiewicz, W.; Galganski, L. Carbon dioxide inhibits COVID-19-type proinflammatory responses through extracellular signal-regulated kinases 1 and 2, novel carbon dioxide sensors. *Cell. Mol. Life Sci.*, 2021; *78:* 8229–8242. [Google Scholar] [CrossRef]
77. Xu, Y.-J.; Elimban, V.; Bhullar, S.K.; Dhalla, N.S. Effects of CO_2 water-bath treatment on blood flow and angiogenesis in ischemic hind limb of diabetic rat. *Can. J. Physiol. Pharmacol.*, 2018; *96:* 1017–1021. [Google Scholar] [CrossRef]
78. Matsumoto, T.; Tanaka, M.; Ikeji, T.; Maeshige, N.; Sakai, Y.; Akisue, T.; Kondo, H.; Ishihara, A.; Fujino, H. Application of transcutaneous carbon dioxide improves capillary regression of skeletal muscle in hyperglycemia. *J. Physiol. Sci.*, 2019; *69:* 317–326. [Google Scholar] [CrossRef]
79. Lahiri, S.; Forster, R.E., 2nd. CO_2/H^+ sensing: Peripheral and central chemoreception. *Int. J. Biochem. Cell Biol.*, 2003; *35:* 1413–1435. [Google Scholar] [CrossRef]
80. Ogoh, S.; Nagaoka, R.; Mizuno, T.; Kimura, S.; Shidahara, Y.; Ishii, T.; Kudoh, M.; Iwamoto, E. Acute vascular effects of carbonated warm water lower leg immersion in healthy young adults. *Physiol. Rep.*, 2016; *4:* e13046. [Google Scholar] [CrossRef]
81. Hill, E.; Dale, N.; Wall, M.J. CO_2-sensitive connexin hemichannels in neurons and glia: Three different modes of signalling? *Int. J. Mol. Sci.*, 2021; *22:* 7254. [Google Scholar] [CrossRef]
82. Reglin, B.; Pries, A.R. Metabolic control of microvascular networks: Oxygen sensing and beyond. *J. Vasc. Res.*, 2014; *51:* 376–392. [Google Scholar] [CrossRef] [PubMed]
83. Németh, B.; Kiss, I.; Ajtay, B.; Péter, I.; Kreska, Z.; Cziráki, A.; Horváth, I.G.; Ajtay, Z. Transcutaneous carbon dioxide treatment is capable of reducing peripheral vascular resistance in hypertensive patients. *Vivo*, 2018; *32:* 1555–1559. [Google Scholar] [CrossRef]
84. Wollina, U.; Heinig, B.; Uhlemann, C. Transdermal CO_2 application in chronic wounds. *Int. J. Low. Extrem Wounds*, 2004; *3:* 103–106. [Google Scholar] [CrossRef] [PubMed]
85. Macura, M.; Ban Frangez, H.; Cankar, K.; Finžgar, M.; Frangez, I. The effect of transcutaneous application of gaseous CO_2 on diabetic chronic wound healing—A double-blind randomized clinical trial. *Int. Wound J.*, 2020; *17:* 1607–1614. [Google Scholar] [CrossRef]
86. Wollina, U.; Heinig, B.; Uhlemann, C. Transdermal CO_2 application in chronic wounds. *Int. J. Low. Extrem Wounds*, 2004; *3:* 103–106. [Google Scholar] [CrossRef] [PubMed]
87. Macura, M.; Ban Frangez, H.; Cankar, K.; Finžgar, M.; Frangez, I. The effect of transcutaneous application of gaseous CO_2 on diabetic chronic wound healing—A double-blind randomized clinical trial. *Int. Wound J.*, 2020; *17:* 1607–1614. [Google Scholar] [CrossRef]
88. Izumi, Y.; Yamaguchi, T.; Yamazaki, T.; Yamashita, N.; Nakamura, Y.; Shiota, M.; Tanaka, M.; Sano, S.; Osada-Oka, M.; Shimada, K.; et al. Percutaneous carbon dioxide treatment using a gas mist generator enhances the collateral blood flow in the ischemic hindlimb. *J. Atheroscl. Thromb.*, 2015; *22:* 38–51. [Google Scholar] [CrossRef]

89. Irie, H.; Tatsumi, T.; Takamiya, M.; Zen, K.; Takahashi, T.; Azuma, A.; Tateishi, K.; Nomura, T.; Hayashi, H.; Nakajima, N.; et al. Carbon dioxide-rich water bathing enhances collateral blood flow in ischemic hindlimb via mobilization of endothelial progenitor cells and activation of NO-cGMP system. *Circulation*, 2005; *111:* 1523–1529. [Google Scholar] [CrossRef] [PubMed]
90. Oe, K.; Ueha, T.; Sakai, Y.; Nikura, T.; Lee, S.Y.; Koh, A.; Hasegawa, T.; Tanaka, M.; Miwa, M.; Kurosaka, M. The effect of transcutaneous application of carbon dioxide (CO_2) on skeletal muscle. *Biochem. Biophys. Res. Commun*, 2011; *407:* 148–152. [Google Scholar] [CrossRef]
91. Hosford, P.S.; Wells, J.A.; Nizari, S.; Christie, I.N.; Theparambil, S.M.; Castro, P.A.; Hadjihambi, A.; Barros, L.F.; Ruminot, I.; Lythgoe, M.F.; et al. CO_2 signaling mediates neurovascular coupling in the cerebral cortex. *Nat. Commun.,* 2022; *13:* 2125. [Google Scholar] [CrossRef]
92. Dospinescu, V.; Nijjar, S.; Spanos, F.; Cook, J.; de Wolf, E.; Biscotti, M.A.; Gerdol, M.; Dale, N. Structural determinants of CO_2-sensitivity in the β connexin family suggested by evolutionary analysis. *Commun. Biol.,* 2019; *2:* 331. [Google Scholar] [CrossRef] [PubMed]
93. Kirby, B.S.; Crecelius, A.R.; Richards, J.C.; Dinenno, F.A. Sources of intravascular ATP during exercise in humans: Critical role for skeletal muscle perfusion. *Exp. Physiol*, 2013; *98:* 988–998. [Google Scholar] [CrossRef] [PubMed]
94. Brayden, J.E. Functional roles of KATP channels in vascular smooth muscle. *Clin. Exp. Pharmacol. Physiol*, 2002; *29:* 312–316. [Google Scholar] [CrossRef]
95. Davies, N.W. Modulation of ATP-sensitive K^+ channels in skeletal muscle by intracellular protons. *Nature*, 1990; *343:* 375–377. [Google Scholar] [CrossRef] [PubMed]
96. Sakai, Y.; Miwa, M.; Oe, K.; Ueha, T.; Koh, A.; Niikura, T.; Iwakura, T.; Lee, S.Y.; Tanaka, M.; Kurosaka, M. A novel system for transcutaneous application of carbon dioxide causing an "artificial bohr effect" in the human body. *PLoS ONE*, 2011; *6:* e24137. [Google Scholar] [CrossRef]
97. Bohr, C.; Hasselbalch, K.; Krogh, A. Ueber einen in biologischer beziehung wichtigen einfluss, den die kohlensäurespannung des blutes auf dessen sauerstoffbindung übt1. *Skandinavisches Archiv Für Physiologie*, 1904; *16:* 402–412. [Google Scholar] [CrossRef]
98. Malte, H.; Lykkeboe, G. The bohr/haldane effect: A model-based uncovering of the full extent of its impact on O_2 delivery to and CO_2 removal from tissues. *J. Appl. Physiol*, 2018; *125:* 916–922. [Google Scholar] [CrossRef]
99. Xu, Y.; Elimban, V.; Dhalla, N.S. Carbon dioxide water-bath treatment augments peripheral blood flow through the development of angiogenesis. *Can. J. Physiol. Pharmacol.*, 2017; *95:* 938–944. [Google Scholar] [CrossRef] [PubMed]
100. Ferrara, N.; Gerber, H.; LeCouter, J. The biology of VEGF and its receptors. *Nat. Med.,* 2003; *9:* 669–676. [Google Scholar] [CrossRef] [PubMed]
101. Selfridge, A.C.; Cavadas, M.A.S.; Scholz, C.C.; Campbell, E.L.; Welch, L.C.; Lecuona, E.; Colgan, S.P.; Barrett, K.E.; Sporn, P.H.S.; Sznajder, J.I.; et al. Hypercapnia suppresses the HIF-dependent adaptive response to hypoxia. *J. Biol. Chem.*, 2016; *291:* 11800–11808. [Google Scholar] [CrossRef]
102. Takemori, T.; Kawamoto, T.; Ueha, T.; Toda, M.; Morishita, M.; Kamata, E.; Fukase, N.; Hara, H.; Fujiwara, S.; Niikura, T.; et al. Transcutaneous carbon dioxide application suppresses bone destruction caused by breast cancer metastasis. *Oncol. Rep.,* 2018; *40:* 2079–2087. [Google Scholar] [CrossRef]
103. Coffey, V.G.; Jemiolo, B.; Edge, J.; Garnham, A.P.; Trappe, S.W.; Hawley, J.A. Effect of consecutive repeated sprint and resistance exercise bouts on acute adaptive responses in human skeletal muscle. *Am. J. Physiol.-Regul. Integr. Comp. Physiol*, 2009; *297:* R1441–R1451. [Google Scholar] [CrossRef]
104. Coffey, V.G.; Hawley, J.A. Concurrent exercise training: Do opposites distract? *J. Physiol.*, 2017; *595:* 2883–2896. [Google Scholar] [CrossRef] [PubMed]
105. Arany, Z.; Foo, S.; Ma, Y.; Ruas, J.L.; Bommi-Reddy, A.; Girnun, G.; Cooper, M.; Laznik, D.; Chinsomboon, J.; Rangwala, S.M.; et al. HIF-independent regulation of VEGF and angiogenesis by the transcriptional coactivator PGC-1α. *Nature*, 2008; *451:* 1008–1012. [Google Scholar] [CrossRef] [PubMed]
106. Haas, T.L.; Lloyd, P.G.; Yang, H.; Terjung, R.L. Exercise Training and Peripheral Arterial Disease. *Compr. Physiol.,* 2012; *2:* 2933–3017. [Google Scholar] [CrossRef]
107. Yan, Z.; Okutsu, M.; Akhtar, Y.N.; Lira, V.A. Regulation of exercise-induced fiber type transformation, mitochondrial biogenesis, and angiogenesis in skeletal muscle. *J. Appl. Physiol.*, 2011; *110:* 264–274. [Google Scholar] [CrossRef]
108. Okamoto, T.; Akita, N.; Kawamoto, E.; Hayashi, T.; Suzuki, K.; Shimaoka, M. Endothelial connexin32 enhances angiogenesis by positively regulating tube formation and cell migration. *Exp. Cell Res.*, 2014; *321:* 133–141. [Google Scholar] [CrossRef]
109. Rahimi, N. The ubiquitin-proteasome system meets angiogenesis. *Mol. Cancer Res.,* 2012; *11:* 538–548. [Google Scholar] [CrossRef]
110. Linthwaite, V.L.; Pawloski, W.; Pegg, H.B.; Townsend, P.D.; Thomas, M.J.; So, V.K.H.; Brown, A.P.; Hodgson, D.R.W.; Lorimer, G.H.; Fushman, D.; et al. Ubiquitin is a carbon dioxide–binding protein. *Sci. Adv.,* 2021; *7:* eabi5507. [Google Scholar] [CrossRef]

111. Deng, M.; Yang, X.; Qin, B.; Liu, T.; Zhang, H.; Guo, W.; Lee, S.; Kim, J.; Yuan, J.; Pei, H.; et al. Deubiquitination and activation of AMPK by USP10. *Mol. Cell.,* 2016; *61:* 614–624. [Google Scholar] [CrossRef]
112. Hardie, D.G.; Ross, F.A.; Hawley, S.A. AMPK: A nutrient and energy sensor that maintains energy homeostasis. *Nat. Rev. Mol. Cell Biol.,* 2012; *13:* 251–262. [Google Scholar] [CrossRef]
113. Cummins, E.P.; Oliver, K.M.; Lenihan, C.R.; Fitzpatrick, S.F.; Bruning, U.; Scholz, C.C.; Slattery, C.; Leonard, M.O.; McLoughlin, P.; Taylor, C.T. NF-κB links CO_2 sensing to innate immunity and inflammation in mammalian cells. *J. Immunol.,* 2010; *185:* 4439–4445. [Google Scholar] [CrossRef]
114. Keogh, C.E.; Scholz, C.C.; Rodriguez, J.; Selfridge, A.C.; von Kriegsheim, A.; Cummins, E.P. Carbon dioxide-dependent regulation of NF-kappaB family members RelB and p100 gives molecular insight into CO_2-dependent immune regulation. *J. Biol. Chem.,* 2017; *292:* 11561–11571. [Google Scholar] [CrossRef] [PubMed]
115. Rodríguez, C.; Muñoz, M.; Contreras, C.; Prieto, D. AMPK, metabolism, and vascular function. *FEBS J.,* 2021; *288:* 3746–3771. [Google Scholar] [CrossRef]